MOLECULAR AND CELLULAR BIOLOGY, Apr. 2008, p. 2332–2341 Vol. 28, No. 7
0270-7306/08/$08.00+0 doi:10.1128/MCB.01490-07

Dyskerin Is a Component of the *Arabidopsis* Telomerase RNP Required for Telomere Maintenance▽

Kalpana Kannan, Andrew D. L. Nelson, and Dorothy E. Shippen*

Department of Biochemistry and Biophysics, Texas A&M University, 2128 TAMU, College Station, Texas 77843-2128

Received 16 August 2007/Returned for modification 11 September 2007/Accepted 8 January 2008

Dyskerin binds the H/ACA box of human telomerase RNA and is a core telomerase subunit required for RNP biogenesis and enzyme function in vivo. Missense mutations in dyskerin result in dyskeratosis congenita, a complex syndrome characterized by bone marrow failure, telomerase enzyme deficiency, and progressive telomere shortening. Here we demonstrate that dyskerin also contributes to telomere maintenance in *Arabidopsis thaliana*. We report that both AtNAP57, the *Arabidopsis* dyskerin homolog, and AtTERT, the telomerase catalytic subunit, accumulate in the plant nucleolus, and AtNAP57 associates with active telomerase RNP particles in an RNA-dependent manner. Furthermore, AtNAP57 interacts in vitro with AtPOT1a, a novel component of *Arabidopsis* telomerase. Although a null mutation in *AtNAP57* is lethal, AtNAP57, like AtTERT, is not haploinsufficient for telomere maintenance in *Arabidopsis*. However, introduction of an *AtNAP57* allele containing a T66A mutation decreased telomerase activity in vitro, disrupted telomere length regulation on individual chromosome ends in vivo, and established a new, shorter telomere length set point. These results imply that T66A NAP57 behaves as a dominant-negative inhibitor of telomerase. We conclude that dyskerin is a conserved component of the telomerase RNP complex in higher eukaryotes that is required for maximal enzyme activity in vivo.

An essential step in the maturation of rRNA is the conversion of uridine to pseudouridine by H/ACA ribonucleoproteins (RNPs) (30). Components of H/ACA RNPs include small nucleolar RNAs (snoRNAs), Gar1, Nhp2, Nop10, and the pseudouridine synthase dyskerin. The dyskerin gene is an essential gene, and its loss results in embryonic lethality in mice (18). In addition to its role in rRNA maturation, dyskerin also binds the H/ACA box of human telomerase RNA (hTR) and is involved in hTR processing and stabilization (6, 32). Mass spectrometry studies indicate that the core telomerase complex is composed of a dimer of a catalytic telomerase reverse transcriptase (TERT), TR (which acts as a template for TERT), and dyskerin (7). Notably, the dyskerin homolog in yeast, Cbf5p, is not stably associated with the telomerase RNA (9), and a different constellation of proteins is required for telomerase RNP biogenesis and enzyme function in this organism (8).

Mutations in human dyskerin are the cause of X-linked dyskeratosis congenita (DC), a rare disease that affects regenerative tissues and is characterized by abnormal skin pigmentation and bone marrow failure (20). Patients suffering from X-linked DC have shorter telomeres than age-matched controls (32). Most mutations in patients with X-linked DC cluster around the PUA (pseudouridine synthase and archeosine transglycosylase) domain of dyskerin, which is responsible for RNA binding (35). One of the most commonly identified dyskerin mutations, A353V, perturbs rRNA pseudouridylation and also results in reduced levels of TR, decreased telomerase activity, and shorter telomeres in mouse embryonic stem cells (33). Similarly, hypomorphic mice that express low levels of dyskerin display the clinical symptoms of DC and exhibit shorter telomeres, but only in later generations (39). While rRNA processing is affected in some dyskerin mutants, the T66A mutation in humans appears to exclusively affect the telomerase-associated functions of dyskerin (32).

Recent data indicate that bone marrow disease can also arise through reduction of other telomerase RNP constituents. Heterozygous mutations in hTR, which reduce its accumulation and perturb its structure, lead to an autosomal dominant form of DC through haploinsufficiency of the RNA subunit (5, 14, 45). Similarly, haploinsufficiency of TERT has been implicated in DC and in aplastic anemia (1, 47, 51). Limiting abundance of telomerase subunits may help to facilitate the fine balance of telomerase repression and activation associated with differentiated cells and their stem cell progenitors (15).

The flowering plant *Arabidopsis thaliana* is a useful model for telomere biology (29). In contrast to those in mice, *Arabidopsis* telomere tracts are relatively short (2 to 5 kb) and are abutted by unique sequences on most chromosome arms (19), making it possible to study the dynamics of individual telomeres. Moreover, *Arabidopsis* is exceptionally tolerant to telomere dysfunction and genome instability. Disruption of At*TERT* results in a slow but progressive loss of telomeric DNA (12). Beginning in the sixth generation (G6), *tert* mutants exhibit a low level of end-to-end chromosome fusions and the onset of growth and developmental defects (37). Remarkably, plants survive for up to five more generations with worsening phenotypes until they ultimately arrest growth in a miniature, dedifferentiated state, unable to produce a germ line (37).

Aside from the presence of AtTERT, little is known about telomerase RNP composition and biogenesis in plants. The TR subunit has not yet been identified in any plant species, owing to the rapid evolution of the TR nucleotide sequence. However, recent studies indicate that AtPOT1a, an oligonucleoti-

* Corresponding author. Mailing address: Texas A&M University, Department of Biochemistry and Biophysics, 2128 TAMU, College Station, Texas 77843-2128. Phone: (979) 862-2342. Fax: (979) 845-9274. E-mail: dshippen@tamu.edu.

▽ Published ahead of print on 22 January 2008.

de-oligosaccharide binding fold (OB-fold)-containing protein whose counterparts in yeast and mammals associate with telomeres (3), functions as a telomerase RNP accessory factor in *Arabidopsis* (43). This observation implies that the composition and/or role of telomerase subunits may vary among higher eukaryotes.

Arabidopsis encodes a dyskerin homolog, At*NAP57* (25, 28), and here we examine its contribution to telomerase biochemistry and telomere maintenance. We demonstrate that AtNAP57 localizes to the nucleolus along with AtTERT and associates with enzymatically active telomerase RNP particles in an RNA-dependent fashion. Although a null mutation is lethal, AtNAP57 is not haploinsufficient for telomere maintenance. However, transgenic plants carrying an At*NAP57* allele with a T66A mutation exhibit decreased telomerase activity in vitro and in vivo, deregulated telomere tracts on individual chromosome ends, and shorter but stable telomeres. We conclude that dyskerin is a conserved component of the telomerase RNP in multicellular organisms that is required for telomere maintenance.

MATERIALS AND METHODS

Plant materials, genotyping, cDNA synthesis, site-directed mutagenesis, and transformation. *Arabidopsis* seeds with T-DNA insertions in the At*NAP57* (SALK_031065) and At*KU70* (SALK_123114) genes were purchased from the *Arabidopsis* Biological Resource Center (Ohio State University, Columbus, OH), cold treated overnight at 4°C, and then placed in an environmental growth chamber and grown under a 16-h light/8-h dark photoperiod at 23°C. *Arabidopsis* suspension culture cells were maintained as described previously (31). Siliques from wild-type and AtNAP57 heterozygotes were dissected 10 days after fertilization and photographed using a Zeiss Axiocam digital camera coupled to a Zeiss microscope.

For genotyping, DNA was extracted from flowers and PCR was performed with the following sets of primers: for At*NAP57*, D5 (5′ GTCGACATCTCAC ACTCGAA 3′) and D8 (5′ GTCTCACTTTGTTCCAGAGT 3′); and for At*KU70*, Ku 1 (5′ TTACTTTGTTGTTTCGGGTGC 3′) and Ku 2 (5′ CTCTT GGCAAGTACACGCTTC 3′).

Total RNA was extracted from 0.5 g of plant tissue using Tri Reagent solution (Sigma). cDNAs were synthesized from total RNA using Superscript III reverse transcriptase (Invitrogen). Oligo(dT) primers were incubated with 2 μg of total RNA in the supplied buffer at 65°C for 5 min. Reverse transcription (RT) was carried out with 100 U of Superscript III at 55°C for 60 min. RNA was degraded with RNase H (USB). For amplification of AtNAP57, we used primers D5 (above) and D2 (5′ GCCATCACAGATGTTGTCATC 3′).

The genomic copy of AtNAP57 (AtNAP57 cDNA plus 1 kb promoter) was amplified by PCR and ligated into a binary vector, pCBK05 (38), lacking the 35S cauliflower mosaic virus promoter. To generate the T66A mutation, site-directed mutagenesis was performed using *Pfu* turbo polymerase (Stratagene) on the genomic version of AtNAP57 in pCBKO5 using the primers M1 (5′ CCTCAA CGTCCGTGCCGGTCAC 3′) and M2 (5′ GTGACCGGCACGGACGTT GAGG 3′) according to the manufacturer's guidelines. The construct was introduced into *Agrobacterium tumefaciens* strain GV3101. Transformation of At*NAP57* heterozygous plants was performed by the in planta method as described in reference 38. Transformants were selected on 0.5 Murashige and Skoog basal medium supplemented with 20 mg/liter of phosphinothricin (Crescent Chemical) and kanamycin (50 μg/ml) and then genotyped. To generate epitope-tagged protein, AtNAP57 cDNA was amplified and ligated into pCBKO5 with an N-terminal 3× FLAG tag. This construct was transformed into *Agrobacterium* and then transformed into wild-type plants as described above.

TRF analysis, PETRA, TRAP, and quantitative TRAP assays. DNA from individual whole plants was extracted, and terminal restriction fragment (TRF) analysis was performed with the Tru1I (Fermentas) restriction enzyme and ^{32}P 5′ end-labeled $(T_3AG_3)_4$ oligonucleotide as a probe (12). The peak value for bulk telomere length (see Fig. 5D) was determined by using ImageQuant software. Primer extension telomere repeat amplification (PETRA) analysis was conducted with DNA from whole plants as described previously (49). Telomere repeat amplification protocol (TRAP) protein extraction and assays were performed with flowers as previously described (11).

Real-time quantitative TRAP was performed as described previously (22) but with the following modifications. A 4.8-ng/μl protein extract dilution (10.5 μl), 1 μl of 10 μM forward primer (5′ CACTATCGACTACGCGATCAG 3′), and 12.5 μl Sybr Green PCR master mix (NEB) were incubated at 37°C for 45 min. One microliter of reverse primer (5′ CCCTAAACCCTAAACCCTAAA 3′) was added, and products were amplified for 35 PCR cycles with 30 s at 95°C and 90 s at 60°C. Threshold cycle values were calculated using an iCycler iQ thermal cycler (Bio-Rad) and the supplied Optical System software. Samples were analyzed in triplicate, with inactivated samples and lysis buffer serving as negative controls.

Western blotting, immunoprecipitation, and immunofluorescence. Plant extracts were made by grinding 0.3 g of flowers in buffer A (50 mM Tris-Cl, pH 7.5, 10 mM $MgCl_2$, 100 mM NaCl, 1 mM EDTA, 10% glycerol, 1 mM dithiothreitol, and plant protease inhibitors [Sigma]). Western blotting was performed with a 1:1,000 dilution of anti-FLAG antibody (Sigma) and a 1:10,000 dilution of horseradish peroxidase-conjugated anti-mouse immunoglobulin G (Sigma). For immunoprecipitation, 50 μl of anti-FLAG beads (Sigma) were washed four times with buffer A and incubated with 500 μl of extract for 2 h at 4°C. Beads were then washed three times with buffer A and eluted using the 3× FLAG peptide for 30 min.

A peptide antibody against AtTERT was raised in rabbits and affinity purified (Covance). The peptide used was N-CIKHKRTLSVHENKRKRDDNVQP, corresponding to residues 180 to 202 of AtTERT. Peptide antibodies against mouse dyskerin (33) were a gift from Monica Bessler.

Arabidopsis suspension culture extracts were made as described above, diluted in buffer W-100 (20 mM TrisOAc [pH 7.5], 10% glycerol, 1 mM EDTA, 5 mM $MgCl_2$, 0.2 M NaCl, 1% NP-40, 0.5 mM sodium deoxycholate, and 100 mM potassium glutamate), and precleared with protein-A agarose (Pierce). Extracts were incubated with antibody and preblocked beads. Beads were washed three times with W-300 (W-100 containing 300 mM potassium glutamate) and once with TMG (10 mM TrisOAc [pH 7.5], 1 mM $MgCl_2$, and 10% glycerol). The beads were then used for either TRAP or Western blotting. Proteins were expressed in rabbit reticulocyte lysate (RRL) (Promega) according to the manufacturer's protocol and used in immunoprecipitation experiments as described above. The fraction of enzymatically active telomerase particles that was associated with AtNAP57 was determined by calculating the efficiency with which the TERT antibody immunoprecipitated telomerase activity in a TRAP assay (relative to input) using ImageQuant software. This value was compared to the amount of AtNAP57 signal obtained by Western blot analysis following immunoprecipitation of these same samples using QuantityOne software.

For immunofluorescence, *Arabidopsis* suspension culture cells and floral buds were fixed with 3.5% formaldehyde in 1× phosphate-buffered saline (PBS) for 30 min and then washed with 1× PBS. Cells were soaked in 1× citric buffer (10 mM sodium citrate and 10 mM EDTA) for 10 min. Citric buffer was removed, and enzyme mix (1% pectinase, 4% cellulose, and 1% macerozyme) was added and incubated at 37°C for 40 min. Cells were rinsed with 1× PBS and spun down onto polylysine-coated slides in a swinging bucket rotor centrifuge for 3 min at 300 × *g*. Slides were removed from the centrifuge and immediately soaked in 1× PBS with 0.2% Triton X-100 for 30 min to make the cells permeable. Slides were washed with 1× PBS and treated with Image-IT solution (Molecular Probes). Primary antibodies (1:200 dilution for AtTERT and 1:400 dilution for dyskerin) were added to the slides, covered with a plastic coverslip, and incubated overnight at room temperature. After washes in 1× PBS and PI buffer (0.2 M NaH_2PO_4, 0.2 M NaOH, and 0.1% IGEPAL CA-630), secondary antibody (goat anti-rabbit immunoglobulin G conjugated to Texas Red 1:200 dilution) was added and incubated for 4 h. Slides were washed, Vectashield containing 4′,6′-diamidino-2-phenylindole (DAPI) was applied, and images were captured using a charged coupled device camera coupled to a Zeiss epifluorescence microscope.

Coimmunoprecipitation and yeast two-hybrid assays. Coimmunoprecipitation was performed as previously described (23) using the full-length AtTERT, AtNAP57, AtKU70, AtKU80, and AtPOT1a proteins expressed in RRL. All components of the yeast two-hybrid system were obtained from Clontech Laboratories. AtNAP57 was subcloned from FLAG-AtNAP57-pCBKO5 into pAS2-1. KU70-pAS2-1, KU80-pAS2-1, and NAP57-pAS2-1 were transformed into the yeast strain AH109. AtKU80 and AtPOT1a were cloned into the prey vector pACT2 and then transformed into the Y187 strain. Yeast mating assays were performed as detailed in the Clontech yeast protocols handbook (no. PT3024-1). Double selection (synthetic dropout medium lacking leucine and tryptophan) was used to obtain diploids, and triple selection (synthetic dropout medium lacking leucine, tryptophan, and histidine) was used to screen for interaction. To confirm interactions, β-galactosidase assays (colony lift filter assay) were performed on the colonies that grew on triple selection plates and development of the blue color was followed for several hours.

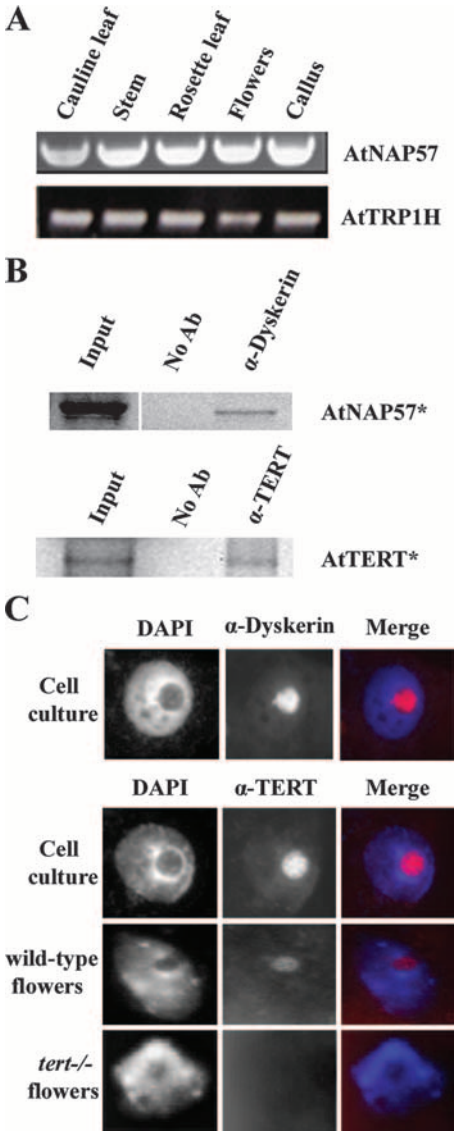

FIG. 1. Expression and localization of AtNAP57. (A) RT-PCR analysis of the AtNAP57 transcript in different plant tissues. AtTRP1H encodes a putative double-strand telomere binding protein (23) and was used as a loading control. (B) Recombinant AtNAP57 and AtTERT proteins were expressed in RRL and labeled with [^{35}S]methionine (*). Proteins were immunoprecipitated with an antibody (Ab) raised against mouse dyskerin (α-dyskerin) or an antibody raised against an N-terminal peptide in AtTERT (α-TERT). Relevant lanes are shown. (C) Immunolocalization of AtNAP57 and AtTERT in *Arabidopsis* suspension culture cells and in floral buds. Nuclei were stained with DAPI or the antibodies discussed above.

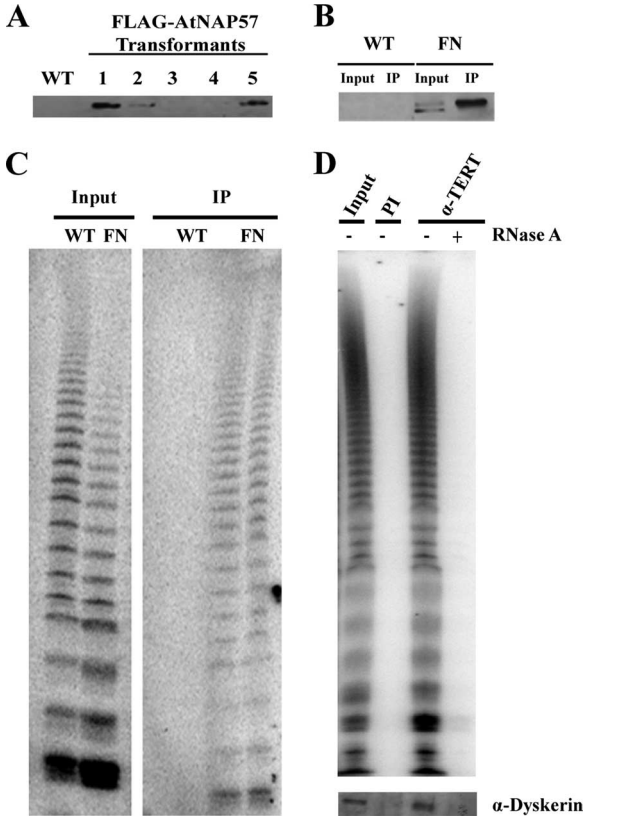

FIG. 2. AtNAP57 associates with *Arabidopsis* telomerase RNP. (A) Western blot analysis with FLAG antibody on plant extracts from the wild type (WT) or transformants bearing FLAG-tagged AtNAP57 (FN). (B) Western blot analysis of input or immunoprecipitates (IP) obtained with FLAG antibody on extracts from the WT and FLAG-tagged AtNAP57 transformants. Four percent of input and 30% of IP was loaded on the gel. (C) TRAP assay results for WT and FN extracts before (input) or after immunoprecipitation (IP) with FLAG antibody. Immunoprecipitates were assayed in duplicate. (D) Top panel, TRAP assay results for cell culture extracts immunoprecipitated with preimmune serum (PI) and anti-TERT (α-TERT) peptide antibody. The sample shown in the far-right lane was pretreated with 100 μg/ml of RNase A prior to immunoprecipitation. Bottom panel, α-TERT immunoprecipitates were subjected to Western blot analysis using the dyskerin antibody (α-dyskerin). Fifteen percent of input and 60% of IP was loaded on the gel.

RESULTS

Characterization of *Arabidopsis* AtNAP57. At*NAP57* is a single-copy gene (At3g57150) on the third *Arabidopsis* chromosome (28) and has only a single exon and no introns. RT-PCR experiments revealed that expression of the 1.6-kb AtNAP57 transcript is ubiquitous (Fig. 1A), as is the case for mammalian dyskerin (16). AtNAP57 mRNA translates to a highly basic protein with a molecular mass of 63 kDa. A heterologous antibody directed at mouse dyskerin (33) immunoprecipitated recombinant AtNAP57 expressed in RRL (Fig. 1B) and the endogenous plant protein (Fig. 2D). This antibody was used to examine the subcellular localization of AtNAP57 in *Arabidopsis* suspension culture cells. Consistent with a role for plant AtNAP57 in rRNA processing, a bright signal for AtNAP57 was detected exclusively in the nucleolus (Fig. 1C). A similar finding was observed by Lermontova et al. in a recent study of *Arabidopsis* dyskerin (25). We next asked whether AtTERT also localized to this compartment, using a peptide antibody raised against AtTERT. The anti-TERT antibody recognized recombinant AtTERT expressed in RRL (Fig. 1B) as well as the endogenous protein from suspension culture extracts (data not shown). Immunolocalization experiments reveal that AtTERT, like AtNAP57, localized to the nucleolus (Fig. 1C). Nucleolar localization of AtTERT was not detected in *tert*$^{-/-}$

flowers, indicating that staining is specific. These findings imply that telomerase biogenesis may occur in the plant nucleolus.

AtNAP57 is a component of *Arabidopsis* telomerase RNP. We asked if AtNAP57 physically associates with *Arabidopsis* telomerase RNP. A fusion construct was generated containing three copies of the FLAG epitope inserted at the N terminus of the AtNAP57 coding region under the control of the robust cauliflower mosaic virus 35S promoter. This construct was transformed into wild-type *Arabidopsis*, and transformants were analyzed by Western blotting using a FLAG antibody. Approximately 1 in 10 of the herbicide-resistant transformants generated detectable levels of the FLAG-AtNAP57 protein (Fig. 2A; data not shown). These plants were used for further study. Complexes containing FLAG-AtNAP57 were immunoprecipitated from transgenic plants and eluted using 3× FLAG peptide. As expected, AtNAP57 was immunoprecipitated from transgenic plants but not from their wild-type counterparts (Fig. 2B).

To monitor AtNAP57 association with telomerase, the TRAP was performed with FLAG-AtNAP57 and wild-type immunoprecipitates. Telomerase activity was immunoprecipitated from FLAG-AtNAP57 plants but not from wild-type plants lacking FLAG-AtNAP57 (Fig. 2C). To verify that the AtNAP57 interaction with telomerase was specific, we performed a reciprocal immunoprecipitation experiment using the TERT peptide antibody to pull down AtNAP57 from suspension culture cell extract. Telomerase activity was immunoprecipitated, and as expected, pretreatment of the extract with RNase A abolished telomerase activity (Fig. 2D). Notably, Western blot analysis revealed a strong enrichment of AtNAP57 in the anti-TERT immunoprecipitate but not when the extract was pretreated with RNase A prior to immunoprecipitation (Fig. 2D, bottom panel). To determine the relative amount of telomerase that was associated with AtNAP57, we compared the efficiency of the AtTERT immunoprecipitate, which was determined to be approximately 10% from the experiment in Fig. 1B, to the amount of AtNAP57 recovered. From these data, we estimate that more than 90% of the active telomerase precipitated by the TERT antibody is associated with AtNAP57. These findings indicate that AtNAP57 is associated with catalytically active telomerase RNP particles and that this interaction requires RNA.

In mammals, dyskerin primarily associates with telomerase through TR. Because TR has not yet been identified in *Arabidopsis*, we examined whether AtNAP57 interacts with the known telomerase-associated proteins in vitro by using coimmunoprecipitation. As expected, in our control reactions (38), we detected the formation of AtKU70-AtKU80 heterodimers, while no interaction was observed for AtKU70 alone (Fig. 3A). We failed to observe binding of T7-tagged AtNAP57 to the radiolabeled full-length TERT protein (Fig. 3A), and similarly, in reciprocal coimmunoprecipitation experiments with T7-tagged AtTERT and labeled AtNAP57, no interaction was detected (data not shown). Furthermore, we did not detect binding of AtNAP57 to segments corresponding to the N terminus, middle, and C terminus of TERT. Although there was a high background level in the AtPOT1a control reaction with beads alone, AtPOT1a abundance was reproducibly higher in the immunoprecipitate of T7-tagged AtNAP57(Fig. 3A; also data not shown). The AtNAP57-POT1a interaction appears to

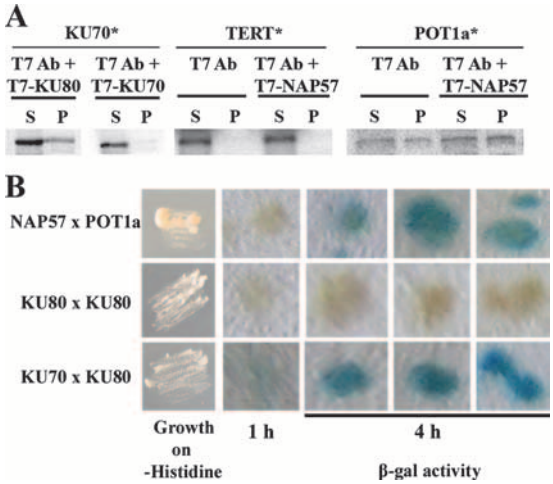

FIG. 3. AtNAP57 weakly associates with AtPOT1a. (A) Coimmunoprecipitation experiments were performed with the full-length recombinant AtKU70, AtTERT, and AtPOT1a proteins, labeled using [^{35}S]methionine (*), and T7-tagged AtKU80, AtKU70, and AtNAP57. Proteins were incubated with either T7 antibody (Ab) beads (control) or T7 beads and the indicated T7-tagged unlabeled proteins. The supernatant (S) and pellet (P) fractions were loaded in equal amounts. (B) Results of yeast two-hybrid analysis are shown. The indicated yeast crosses were performed and plated on medium lacking leucine, tryptophan, and histidine. Results of a colony lift β-galactosidase (β-gal) assay are shown. The blue color is indicative of protein interaction.

be specific since a closely related protein, AtPOT1b (40), was not precipitated with T7-tagged AtNAP57 (data not shown). We confirmed the AtNAP57-AtPOT1a interaction using a yeast two-hybrid mating assay. Yeast strains containing different plasmids were mated, and diploids were selected by triple selection (Fig. 3B). To monitor reporter gene activity, β-galactosidase assays were performed. Blue staining, indicative of interaction, was observed for AtKU70-AtKU80 within 1 h, and after 4 h, staining was detected for AtNAP57-AtPOT1a (Fig. 3B). Thus, the interaction between AtNAP57 and AtPOT1a is weak but specific. Taken together, these data argue that AtNAP57 is physically associated with the *Arabidopsis* telomerase RNP.

AtNAP57 is not haploinsufficient for telomere maintenance in *Arabidopsis*. To investigate the role of AtNAP57 in telomere maintenance, we obtained a mutant line (SALK_031065) carrying a T-DNA insertion in the extreme 5′ end of the gene corresponding to the 18th amino acid of the AtNAP57 open reading frame (Fig. 4A). Although we genotyped a population of more than 50 progeny from this line, we did not recover any homozygous mutants (data not shown). Dissection of siliques (seed pods) from the heterozygous mutants revealed a reduced seed set in which approximately 25% of the seeds failed to form viable embryos (Fig. 4B). This outcome implies that AtNAP57 is an essential gene, a conclusion consistent with a recent report for plants with homozygous mutation in AtNAP57 (25).

Heterozygous AtNAP57 mutants were indistinguishable from the wild type in their growth and development over successive plant generations. Furthermore, TRF analysis conducted on 10 first-generation (G1) *nap57*$^{+/-}$ mutants revealed

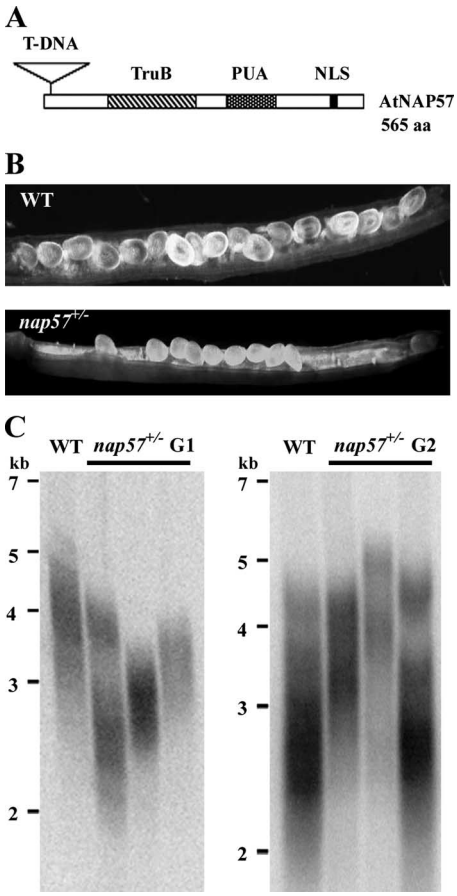

FIG. 4. At*NAP57* is an essential gene in *Arabidopsis*. (A) Schematic diagram of the At*NAP57* coding region showing the position of the T-DNA insertion, pseudouridine synthase domain (TruB), pseudouridine synthase, archeosine transglycosylase domain (PUA), and nuclear localization signal (NLS). (B) Siliques (seed pods) from wild-type (WT) or *nap57*$^{+/-}$ plants were visualized by microscopy. A reduced seed set was observed for *nap57*$^{+/-}$ plants, implying that the homozygous mutation is lethal. (C) TRF analysis of WT, first-generation (G1), or second-generation (G2) *nap57*$^{+/-}$ plants. Molecular size markers are indicated.

some variability in bulk telomere length, but in all cases, telomeres were in the wild-type 2- to 5-kb size range (Fig. 4C, left panel; also data not shown). A similar result was obtained when telomeres from G2 *nap57*$^{+/-}$ mutants were examined (Fig. 4C, right panel; data not shown). These data imply that AtNAP57 is not haploinsufficient for telomere length maintenance in *Arabidopsis*.

The T66A mutation in AtNAP57 results in a new, shorter telomere length set point. The T66A missense mutation in dyskerin culminates in DC in humans and is associated with a defect in telomere maintenance (32). Since threonine 66 is conserved in AtNAP57 (Fig. 5A), we asked whether an alanine substitution at this site would lead to a telomere-related phenotype in plants. Plants heterozygous for the T-DNA insertion in At*NAP57* were transformed with an At*NAP57* gene carrying the T66A mutation under the control of its native promoter (Fig. 5B). We expected to obtain plants heterozygous or homozygous with respect to the T-DNA insertion and which also carried exogenous T66A NAP57. Surprisingly, we failed to recover plants that were homozygous for the T-DNA insertion in At*NAP57* and also contained the T66A transgene. Thus, the At*NAP57* gene bearing the T66A mutation is unable to rescue plants homozygous for the T-DNA insertion.

To test the effect of T66A NAP57 on bulk telomere length, TRF analysis was performed on the first generation of transformants expressing T66A NAP57 (T1). Based on previous transformation experiments (Fig. 2) (42, 49), we expected that any detrimental consequences of the T66A mutation would be evident in a population of 10 to 20 transformants (T1 generation). Accordingly, we examined 20 independent transgenic lines. While for most plants bulk telomeres were in the wild-type range (Fig. 5C, lanes 2 and 3; data not shown), a subset of telomeres in several plants were significantly shorter than wild-type telomeres and their shortest telomere tracts trailed down to below 1.6 kb in length (Fig. 5C, lanes 4 and 5). To determine whether telomeres would continue to shorten in subsequent generations, we monitored the progeny of one T1 plant (Fig. 5C, lane 4, and D). For all of the T2 progeny, the shortest telomere tracts migrated below 2 kb (Fig. 5C, lanes 7 to 10), and for one plant, the range of telomere lengths was nearly identical to that for its T1 parent, spanning ~1.2 to 3.5 kb (Fig. 5C, compare lanes 4 and 7). When this T2 plant was propagated to T3, the telomere tracts of all four progeny were of similar lengths to those of their T2 parent (Fig. 5C, lanes 12 to 15, and D). The loss of longer telomeres was more pronounced in T3 plants (Fig. 5D). The average bulk telomere length in wild-type plants (~4 kb) was reduced by 2 kb in T3 T66A mutants to ~2.1 kb (Fig. 5D). We detected no additional shortening in two T4 plants monitored (data not shown). Furthermore, none of the shortest telomeres fell below 1 kb in the four generations the transgenic plants were propagated (Fig. 5D). Thus, the T66A mutation perturbs telomere length regulation but does not result in progressive telomere shortening. Instead, this mutation appears to promote the establishment of a new, shorter length set point.

The T66A mutation in AtNAP57 deregulates telomere length on individual chromosome ends. To further examine telomere length dynamics in T66A *nap57* mutants, we monitored telomeres on three individual chromosome arms, the right arm of chromosome 2, the left arm of chromosome 3, and the right arm of chromosome 4, using PETRA. As expected, PETRA produced a single diffuse band for each telomere in wild-type samples (Fig. 6A, lanes 1 to 3), consistent with tight regulation of telomere tracts on homologous chromosomes (41). A similar profile was observed with *nap57*$^{+/-}$ mutants (Fig. 6A, lanes 4 to 6). A different result was obtained with T66A *nap57* mutants. In the T1, T2, and T3 mutants that displayed shorter bulk telomere lengths, individual telomere tracts appeared as a cluster of several sharp bands (Fig. 6A, lanes 10 to 18; Fig. 6B). In contrast, the siblings of these plants whose bulk telomeres fell within the wild-type range showed a PETRA profile that more closely resembled that of wild-type plants (Fig. 6A, lanes 7 to 9; Fig. 6B). This finding implies that telomere length regulation on homologous chromosomes is perturbed in T66A *nap57* mutants. As discussed below, this phenotype is consistent with decreased telomerase activity.

The T66A mutation in AtNAP57 decreases telomerase activity in vitro and in vivo. To determine whether the T66A mutation in AtNAP57 decreased telomerase enzyme activity in

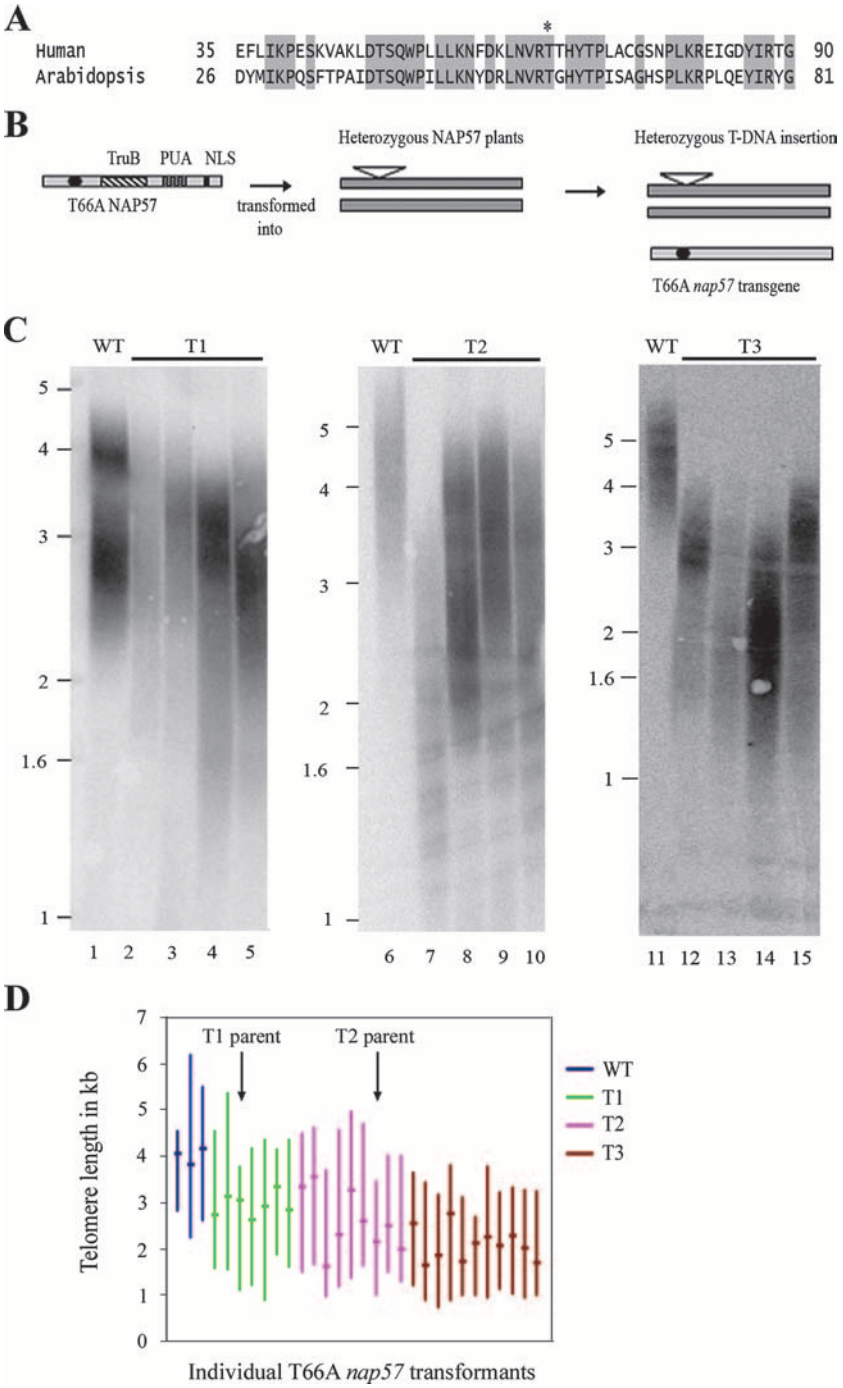

FIG. 5. The T66A mutation in AtNAP57 results in the establishment of a shorter telomere length set point. (A) Sequence alignment of human dyskerin and AtNAP57 proteins. Conserved residues are highlighted in gray boxes, and the threonine residue targeted for mutagenesis is denoted by an asterisk. (B) Overview of the process for introduction of the T66A mutation in AtNAP57 into *nap57*$^{+/-}$ plants. (C) TRF analysis of first, second, and third (T1, T2, and T3) generations of T66A transformants. The T1 plant whose telomeres were analyzed in the left panel, lane 4, was used as the parent for T2 progeny plants analyzed in the middle panel. The T2 plant represented in the middle panel, lane 7, was the parent for the T3 progeny analyzed in the right panel. DNA samples were not run as far into the gel shown the right panel as in the other two gels. (D) Graphic representation of bulk telomere length size range and peak telomere length (indicated by -) for WT and T66A transformants is shown. Arrows indicate telomere length measurements for plants used as T1 and T2 parents.

vitro, a TRAP assay was performed. Extract titration experiments revealed no detectable difference in the level of telomerase activity for the wild type versus that for *nap57*$^{+/-}$ mutants (Fig. 6C), supporting the conclusion that AtNAP57 is not haploinsufficient in *Arabidopsis*. In contrast, TRAP conducted at the highest dilution (1:5,000) of protein extract reproducibly revealed decreases in vitro telomerase activity for T66A transformants relative to levels for *nap57*$^{+/-}$ siblings (Fig. 6C). To

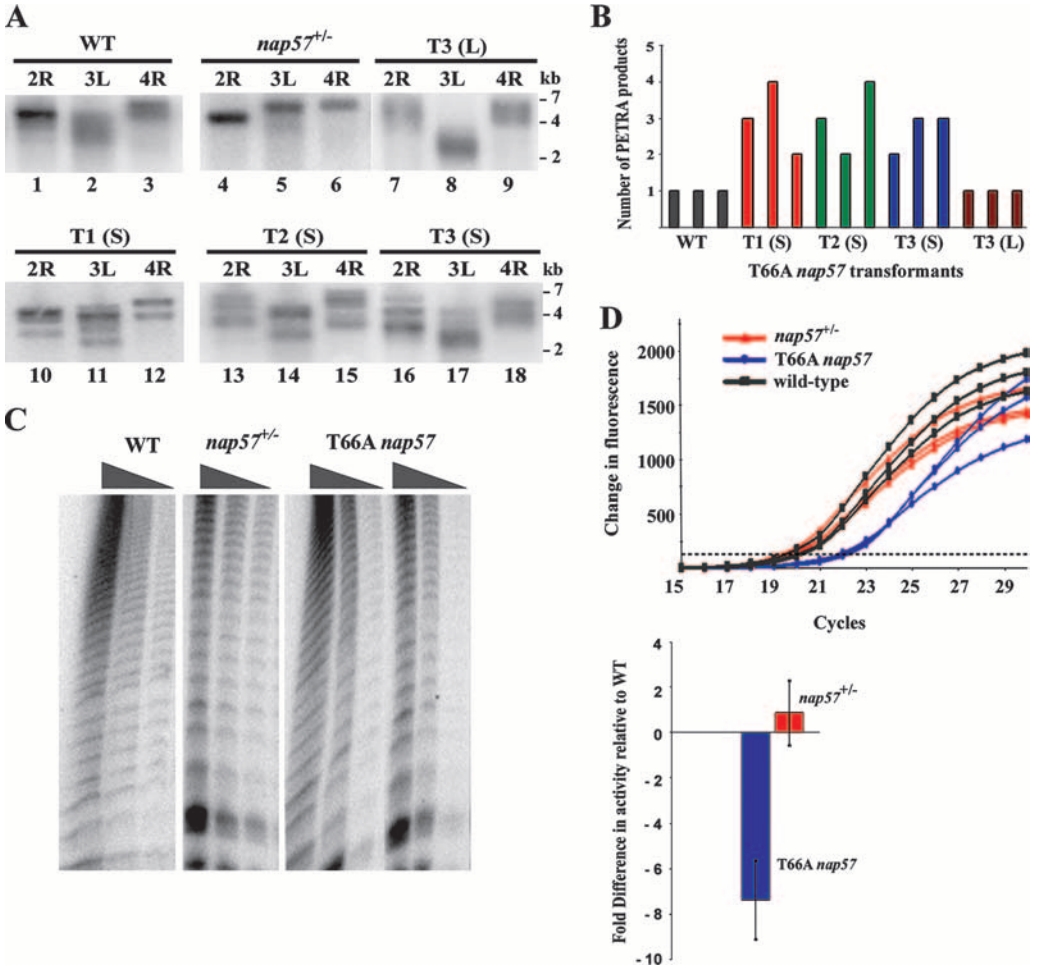

FIG. 6. The T66A mutation in AtNAP57 affects telomere length regulation on individual chromosome ends and decreases telomerase activity in vitro. (A) PETRA results are shown for the WT and individual *nap57*$^{+/-}$, T1, T2, and T3 T66A *nap57* transformants with short telomeres (S) and a T3 T66A *nap57* transformant with wild-type-length telomeres (L). The telomeres monitored are indicated. 2R, right arm of chromosome 2; 3L, left arm of chromosome 3; 4R, right arm of chromosome 4. (B) Graphic representation of PETRA products obtained in each reaction as determined by visual inspection. (C) TRAP assay results for the WT and *nap57*$^{+/-}$ and T66A *nap57* transformants. Reactions were conducted using 1:50, 1:500, and 1:5,000 dilutions of protein extracts. (D) Results of real-time TRAP. The top panel shows raw data for three (each) of the WT and *nap57*$^{+/-}$ and T66A *nap57* transformants. The dashed line represents the threshold cycle for TRAP product detection. The bottom panel shows a histogram of the telomerase activity levels for *nap57*$^{+/-}$ and T66A transformants relative to those for the WT. Extracts from 10 individual plants from each genotype were monitored.

more precisely gauge the level of telomerase activity in these mutants, we performed quantitative real-time TRAP following a method developed to monitor telomerase activity levels in human cells (22). As expected, we found no significant difference in telomerase activity in extracts prepared from *nap57*$^{+/-}$ plants versus those from wild-type plants. In contrast, T66A *nap57* mutants showed a sevenfold decrease in enzyme activity (Fig. 6D).

To examine the effect of the T66A *nap57* mutation on telomerase activity in vivo, we studied the consequences of this mutation in *ku70* mutants. KU70 is best known for its role in the nonhomologous-end-joining DNA repair pathway (36), but in *Arabidopsis* it also acts as a potent negative regulator of telomerase (13, 38). Telomeres in *ku70* mutants expand to two- to threefold the size of wild-type telomeres in a single generation, and this elongation is dependent on telomerase (38, 49). Thus, we predicted that incorporation of T66A *nap57* into the telomerase RNP would diminish the enzyme's ability to elongate telomeres in a *ku70* background. To test this hypothesis, we crossed the T66A *nap57* transformants with *ku70*$^{-/-}$ plants (Fig. 7A). In the first (F1) generation, we generated plants heterozygous for At*KU70* and At*NAP57* and selected for the T66A mutant transgene. In the second generation (F2), we recovered plants that were *ku70*$^{-/-}$ *nap57*$^{+/-}$ and carried the mutant T66A transgene. TRF analysis of the F2 population showed that *ku70*$^{-/-}$ *nap57*$^{+/-}$ plants elongated their telomeres to 5 to 8 kb (Fig. 7B, lane 8) while telomeres remained short in the presence of the T66A transgene (Fig. 7B, lanes 1 to 7). We conclude that expression of the T66A *nap57* allele prevents telomerase from hyperelongating telomeres when its negative regulator, *KU70*, is inactivated. Altogether, our data argue that AtNAP57 is essential for maximal activity of the *Arabidopsis* telomerase RNP in vivo.

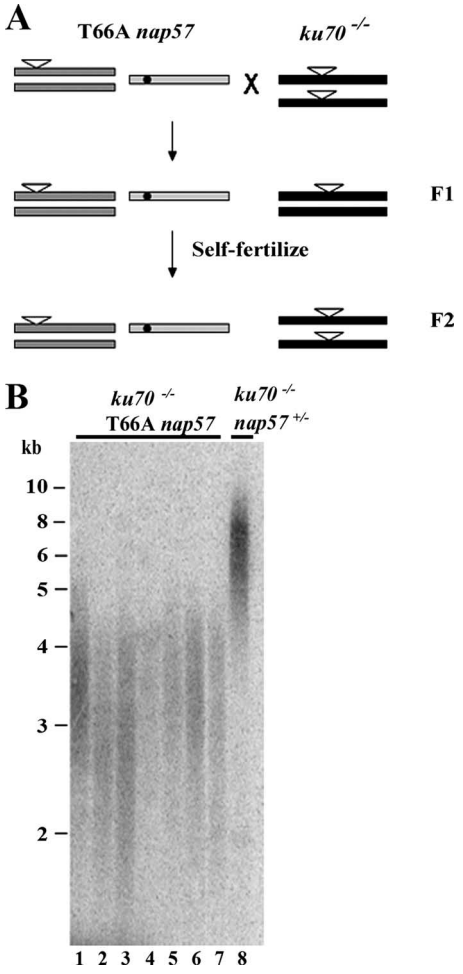

FIG. 7. The T66A mutation in AtNAP57 reduces telomerase activity in vivo. (A) Schematic diagram of genetic crossing scheme to generate $ku70^{-/-}$ mutants carrying the T66A *nap57* allele. (B) TRF analysis of seven $ku70^{-/-}$ T66A *nap57* plants and one $ku70^{-/-}$ $nap57^{+/-}$ control plant is shown.

DISCUSSION

A conserved pathway for telomerase biogenesis in higher eukaryotes. The telomerase RNP is evolving at a rapid pace. The TR and TERT subunits have diverged dramatically, and a distinct set of proteins has emerged in higher and lower eukaryotes to promote RNP biogenesis and enzyme action at the chromosome terminus (6, 8). The yeast TR (TLC1) bears an Sm protein binding motif and has adopted an RNP biogenesis scheme similar to that of snRNPs (40), while vertebrate TRs have acquired a 3′ H/ACA box domain found in snoRNAs and are bound by the dyskerin complex. Thus, although dyskerin's function in catalyzing pseudouridylation of ribosomal RNAs is conserved, in mammals it has evolved an additional, more specialized role as an integral component of the telomerase RNP (7, 32).

In this report, we provide several lines of evidence that telomerase enzymes from higher eukaryotes share a requirement for dyskerin. First, we found that the AtNAP57 and AtTERT proteins colocalize to the nucleolus in *Arabidopsis*. Nucleolar localization of telomerase could be especially advantageous for *Arabidopsis*, since telomeres cluster at the nucleolar periphery (2). Second, we showed that AtNAP57 physically associates with enzymatically active telomerase particles. The major interaction partner for AtNAP57 in the plant telomerase RNP is likely to be TR, since association of AtNAP57 with telomerase is abolished following RNase A treatment. Intriguingly, we also discovered a novel but weak interaction for AtNAP57 with AtPOT1a. AtPOT1a is an OB-fold–bearing protein that physically interacts with catalytically active telomerase in *Arabidopsis* and promotes enzyme function in vitro and in vivo (43). Recent studies indicate that human telomerase associates with TPP1, an hPOT1 binding partner that also harbors an OB-fold motif (48, 50). Whether the human dyskerin contacts TPP1 is unknown. Third, and most importantly, we demonstrated that AtNAP57 is crucial for the function of *Arabidopsis* telomerase. Transgenic plants bearing a mutant AtNAP57 allele display reduced levels of telomerase activity in vitro and perturbed telomere length regulation in vivo (see below).

***Arabidopsis* is not haploinsufficient for its known telomerase components.** Essential components of the telomerase RNP are limiting in mammals and yeast. In both $terc^{+/-}$ (TR) and $tert^{+/-}$ embryonic stem mouse cells, telomere maintenance is compromised (10, 17, 27). Indeed, haploinsufficiency of hTR is directly linked to autosomal dominant DC, and the reduced hTR levels along with shorter telomeres in these patients result in disease anticipation (46). Similarly, recent studies indicate that TLC1, the TR component in *Saccharomyces cerevisiae*, is haploinsufficient for telomere maintenance (34). Moreover, yeast heterozygous for both TLC1 and EST1, a telomerase-associated protein, exhibit a phenomenon referred to as additive haploinsufficiency, where telomere tracts are even shorter than those in either single heterozygote (24, 26).

In contrast, the known telomerase-associated proteins in *Arabidopsis*, AtTERT (12), AtPOT1a (43), and AtNAP57 (this study), are not haploinsufficient for telomere maintenance. Plants heterozygous for these components display wild-type levels of telomerase activity in vitro and maintain telomeres in the wild-type size range through multiple generations. While it is possible that TR will prove to be present in limiting quantities, *Arabidopsis* may simply require a very low level of telomerase to maintain genome stability. We note that the *Arabidopsis* genome is comprised of only 10 chromosomes (20 telomeres), significantly fewer than in diploid budding yeast (64 telomeres) or in human (92 telomeres) cells.

The T66A mutation in AtNAP57 acts as a dominant-negative allele to decrease telomerase activity in vitro and in vivo. The T66A mutation in human dyskerin leads to DC through reduction in the steady-state level of hTR, decreased telomerase activity, and progressive telomere shortening (32). To determine if *Arabidopsis* would exhibit similar defects in telomerase, we generated transgenic plants harboring the corresponding mutant allele. As for humans (32), the T66A mutation in AtNAP57 did not grossly affect rRNA processing in *Arabidopsis* (K. Kannan and D. Shippen, unpublished data). Nonetheless, this mutation is highly deleterious; expression of this allele could not rescue the lethality associated with plants lacking both copies of wild-type AtNAP57. Furthermore, although plants harboring one wild-type copy of At*NAP57* and the T66A *nap57* transgene were viable, they displayed de-

creased telomerase activity both in vitro and in vivo. We suspect that this outcome is a consequence of reduced stability of telomerase RNA, but testing of this hypothesis awaits identification of this molecule. Nonetheless, in marked contrast to the fate of human telomeres in T66A DC cells (32), telomeres in T66A *nap57* transgenic plants did not undergo progressive shortening. Instead, telomeres were stably maintained at a length approximately 2 kb shorter than that in the wild type.

Data from PETRA on individual chromosome ends argue that this new length set point for telomeres is a consequence of limiting telomerase activity. In the PETRA assay, wild-type telomeres on homologous chromosomes typically appear as a single heterogeneous band (Fig. 6A) (41). Because DNA from an entire plant is analyzed, these results mean that individual telomere tracts are subjected to extremely tight regulation during plant growth and development (39). Strikingly, with T66A *nap57* mutants, PETRA generates a complex profile of multiple sharp bands, indicating that telomere length is deregulated on individual chromosome ends. Previous studies with yeast (44), mammals (21), and *Arabidopsis* (41) show that telomerase acts preferentially on the shortest telomeres in the population. We hypothesize that substrate preference is exacerbated in plants with reduced levels of telomerase (e.g., T66A *nap57* mutants), resulting in elongation of only a subset of telomeres in a fraction of cells. Bulk telomeres can then establish a new length set point when equilibrium between the compromised telomerase and forces that shorten telomeres (e.g., the end replication problem, nuclease action, and recombination) is attained. Because the demand for telomerase activity is significantly greater in humans, we suspect such cells bearing the T66A *nap57* mutation fail to achieve a new telomere length set point and suffer progressive telomere erosion.

How does the T66A mutation in AtNAP57 inhibit telomerase activity in *Arabidopsis*? Since AtNAP57 is not haploinsufficient for telomerase function in plants but telomerase is inhibited when the T66A *nap57* allele is introduced into this background, the data argue that T66A NAP57 acts as a dominant-negative inhibitor. Catalytically active human telomerase is a 670-kDa dimer comprised of two TERT, two TR, and two dyskerin molecules (7). *Arabidopsis* telomerase has approximately the same molecular mass, and like hTERT (4), AtTERT is capable of dimerization in vitro (C. Cifuentes-Rojas, K. Kannan, and D. Shippen, unpublished data). Thus, the plant telomerase may also harbor two copies of AtNAP57. Accordingly, incorporation of a mutant form of this protein into the telomerase RNP may compromise enzyme function.

ACKNOWLEDGMENTS

We are grateful to Monica Bessler for providing the mouse dyskerin antibody, Keerti Rathore, Sunilkumar Ganesan, and Jon Lamb for help with microscopy and immunofluorescence, Laurent Vespa for help with the plant crosses, Eugene Shakirov for providing *Arabidopsis* suspension culture cells for analysis, and Erin Gentry and Brittney-Shea Herbert for their assistance with quantitative TRAP. We also thank members of the Shippen lab for insightful discussions and Brijesh Rao for assistance with data analysis.

This work was supported by grants from NSF (MCB0235987) and NIH (GM065383) to D.E.S.

REFERENCES

1. **Armanios, M., J. L. Chen, Y. P. Chang, R. A. Brodsky, A. Hawkins, C. A. Griffin, J. R. Eshleman, A. R. Cohen, A. Chakravarti, A. Hamosh, and C. W. Greider.** 2005. Haploinsufficiency of telomerase reverse transcriptase leads to anticipation in autosomal dominant dyskeratosis congenita. Proc. Natl. Acad. Sci. USA **102:**15960–15964.
2. **Armstrong, S. J., F. C. Franklin, and G. H. Jones.** 2001. Nucleolus-associated telomere clustering and pairing precede meiotic chromosome synapsis in Arabidopsis thaliana. J. Cell Sci. **114:**4207–4217.
3. **Baumann, P.** 2006. Are mouse telomeres going to pot? Cell **126:**33–36.
4. **Beattie, T. L., W. Zhou, M. O. Robinson, and L. Harrington.** 2001. Functional multimerization of the human telomerase reverse transcriptase. Mol. Cell. Biol. **21:**6151–6160.
5. **Cerone, M. A., R. J. Ward, J. A. Londono-Vallejo, and C. Autexier.** 2005. Telomerase RNA mutated in autosomal dyskeratosis congenita reconstitutes a weakly active telomerase enzyme defective in telomere elongation. Cell Cycle **4:**585–589.
6. **Chen, J. L., and C. W. Greider.** 2004. Telomerase RNA structure and function: implications for dyskeratosis congenita. Trends Biochem. Sci. **29:**183–192.
7. **Cohen, S. B., M. E. Graham, G. O. Lovrecz, N. Bache, P. J. Robinson, and R. R. Reddel.** 2007. Protein composition of catalytically active human telomerase from immortal cells. Science **315:**1850–1853.
8. **Collins, K.** 2006. The biogenesis and regulation of telomerase holoenzymes. Nat. Rev. Mol. Cell Biol. **7:**484–494.
9. **Dez, C., A. Henras, B. Faucon, D. Lafontaine, M. Caizergues-Ferrer, and Y. Henry.** 2001. Stable expression in yeast of the mature form of human telomerase RNA depends on its association with the box H/ACA small nucleolar RNP proteins Cbf5p, Nhp2p and Nop10p. Nucleic Acids Res. **29:**598–603.
10. **Erdmann, N., Y. Liu, and L. Harrington.** 2004. Distinct dosage requirements for the maintenance of long and short telomeres in mTert heterozygous mice. Proc. Natl. Acad. Sci. USA **101:**6080–6085.
11. **Fitzgerald, M. S., T. D. McKnight, and D. E. Shippen.** 1996. Characterization and developmental patterns of telomerase expression in plants. Proc. Natl. Acad. Sci. USA **93:**14422–14427.
12. **Fitzgerald, M. S., K. Riha, F. Gao, S. Ren, T. D. McKnight, and D. E. Shippen.** 1999. Disruption of the telomerase catalytic subunit gene from Arabidopsis inactivates telomerase and leads to a slow loss of telomeric DNA. Proc. Natl. Acad. Sci. USA **96:**14813–14818.
13. **Gallego, M. E., J. Y. Bleuyard, S. Daoudal-Cotterell, N. Jallut, and C. I. White.** 2003. Ku80 plays a role in non-homologous recombination but is not required for T-DNA integration in Arabidopsis. Plant J. **35:**557–565.
14. **Goldman, F., R. Bouarich, S. Kulkarni, S. Freeman, H. Y. Du, L. Harrington, P. J. Mason, A. Londono-Vallejo, and M. Bessler.** 2005. The effect of TERC haploinsufficiency on the inheritance of telomere length. Proc. Natl. Acad. Sci. USA **102:**17119–17124.
15. **Harrington, L.** 2005. Making the most of a little: dosage effects in eukaryotic telomere length maintenance. Chromosome Res. **13:**493–504.
16. **Hassock, S., D. Vetrie, and F. Giannelli.** 1999. Mapping and characterization of the X-linked dyskeratosis congenita (DKC) gene. Genomics **55:**21–27.
17. **Hathcock, K. S., M. T. Hemann, K. K. Opperman, M. A. Strong, C. W. Greider, and R. J. Hodes.** 2002. Haploinsufficiency of mTR results in defects in telomere elongation. Proc. Natl. Acad. Sci. USA **99:**3591–3596.
18. **He, J., S. Navarrete, M. Jasinski, T. Vulliamy, I. Dokal, M. Bessler, and P. J. Mason.** 2002. Targeted disruption of Dkc1, the gene mutated in X-linked dyskeratosis congenita, causes embryonic lethality in mice. Oncogene **21:**7740–7744.
19. **Heacock, M., E. Spangler, K. Riha, J. Puizina, and D. E. Shippen.** 2004. Molecular analysis of telomere fusions in Arabidopsis: multiple pathways for chromosome end-joining. EMBO J. **23:**2304–2313.
20. **Heiss, N. S., S. W. Knight, T. J. Vulliamy, S. M. Klauck, S. Wiemann, P. J. Mason, A. Poustka, and I. Dokal.** 1998. X-linked dyskeratosis congenita is caused by mutations in a highly conserved gene with putative nucleolar functions. Nat. Genet. **19:**32–38.
21. **Hemann, M. T., M. A. Strong, L. Y. Hao, and C. W. Greider.** 2001. The shortest telomere, not average telomere length, is critical for cell viability and chromosome stability. Cell **107:**67–77.
22. **Herbert, B. S., A. E. Hochreiter, W. E. Wright, and J. W. Shay.** 2006. Nonradioactive detection of telomerase activity using the telomeric repeat amplification protocol. Nat. Protoc. **1:**1583–1590.
23. **Karamysheva, Z. N., Y. V. Surovtseva, L. Vespa, E. V. Shakirov, and D. E. Shippen.** 2004. A C-terminal Myb extension domain defines a novel family of double-strand telomeric DNA-binding proteins in Arabidopsis. J. Biol. Chem. **279:**47799–47807.
24. **Lendvay, T. S., D. K. Morris, J. Sah, B. Balasubramanian, and V. Lundblad.** 1996. Senescence mutants of Saccharomyces cerevisiae with a defect in telomere replication identify three additional EST genes. Genetics **144:**1399–1412.
25. **Lermontova, I., V. Schubert, F. Bornke, J. Macas, and I. Schubert.** 2007. Arabidopsis CBF5 interacts with the H/ACA snoRNP assembly factor NAF1. Plant Mol. Biol. **65:**615–626.
26. **Lingner, J., T. R. Cech, T. R. Hughes, and V. Lundblad.** 1997. Three Ever Shorter Telomere (EST) genes are dispensable for in vitro yeast telomerase activity. Proc. Natl. Acad. Sci. USA **94:**11190–11195.
27. **Liu, Y., H. Kha, M. Ungrin, M. O. Robinson, and L. Harrington.** 2002.

Preferential maintenance of critically short telomeres in mammalian cells heterozygous for mTert. Proc. Natl. Acad. Sci. USA **99:**3597–3602.
28. **Maceluch, J., M. Kmieciak, Z. Szweykowska-Kulinska, and A. Jarmolowski.** 2001. Cloning and characterization of Arabidopsis thaliana AtNAP57—a homologue of yeast pseudouridine synthase Cbf5p. Acta Biochim. Pol. **48:** 699–709.
29. **McKnight, T. D., and D. E. Shippen.** 2004. Plant telomere biology. Plant Cell **16:**794–803.
30. **Meier, U. T.** 2005. The many facets of H/ACA ribonucleoproteins. Chromosoma **114:**1–14.
31. **Menges, M., and J. A. Murray.** 2002. Synchronous Arabidopsis suspension cultures for analysis of cell-cycle gene activity. Plant J. **30:**203–212.
32. **Mitchell, J. R., E. Wood, and K. Collins.** 1999. A telomerase component is defective in the human disease dyskeratosis congenita. Nature **402:**551–555.
33. **Mochizuki, Y., J. He, S. Kulkarni, M. Bessler, and P. J. Mason.** 2004. Mouse dyskerin mutations affect accumulation of telomerase RNA and small nucleolar RNA, telomerase activity, and ribosomal RNA processing. Proc. Natl. Acad. Sci. USA **101:**10756–10761.
34. **Mozdy, A. D., and T. R. Cech.** 2006. Low abundance of telomerase in yeast: implications for telomerase haploinsufficiency. RNA **12:**1721–1737.
35. **Rashid, R., B. Liang, D. L. Baker, O. A. Youssef, Y. He, K. Phipps, R. M. Terns, M. P. Terns, and H. Li.** 2006. Crystal structure of a Cbf5-Nop10-Gar1 complex and implications in RNA-guided pseudouridylation and dyskeratosis congenita. Mol. Cell **21:**249–260.
36. **Riha, K., M. L. Heacock, and D. E. Shippen.** 2006. The role of the nonhomologous end-joining DNA double-strand break repair pathway in telomere biology. Annu. Rev. Genet. **40:**237–277.
37. **Riha, K., T. D. McKnight, L. R. Griffing, and D. E. Shippen.** 2001. Living with genome instability: plant responses to telomere dysfunction. Science **291:**1797–1800.
38. **Riha, K., J. M. Watson, J. Parkey, and D. E. Shippen.** 2002. Telomere length deregulation and enhanced sensitivity to genotoxic stress in Arabidopsis mutants deficient in Ku70. EMBO J. **21:**2819–2826.
39. **Ruggero, D., S. Grisendi, F. Piazza, E. Rego, F. Mari, P. H. Rao, C. Cordon-Cardo, and P. P. Pandolfi.** 2003. Dyskeratosis congenita and cancer in mice deficient in ribosomal RNA modification. Science **299:**259–262.
40. **Seto, A. G., A. J. Zaug, S. G. Sobel, S. L. Wolin, and T. R. Cech.** 1999. Saccharomyces cerevisiae telomerase is an Sm small nuclear ribonucleoprotein particle. Nature **401:**177–180.
41. **Shakirov, E. V., and D. E. Shippen.** 2004. Length regulation and dynamics of individual telomere tracts in wild-type Arabidopsis. Plant Cell **16:**1959–1967.
42. **Shakirov, E. V., Y. V. Surovtseva, N. Osbun, and D. E. Shippen.** 2005. The Arabidopsis Pot1 and Pot2 proteins function in telomere length homeostasis and chromosome end protection. Mol. Cell. Biol. **25:**7725–7733.
43. **Surovtseva, Y. V., E. V. Shakirov, L. Vespa, N. Osbun, X. Song, and D. E. Shippen.** 2007. Arabidopsis POT1 associates with the telomerase RNP and is required for telomere maintenance. EMBO J. **26:**3653–3661.
44. **Teixeira, M. T., M. Arneric, P. Sperisen, and J. Lingner.** 2004. Telomere length homeostasis is achieved via a switch between telomerase-extendible and -nonextendible states. Cell **117:**323–335.
45. **Vulliamy, T., A. Marrone, F. Goldman, A. Dearlove, M. Bessler, P. J. Mason, and I. Dokal.** 2001. The RNA component of telomerase is mutated in autosomal dominant dyskeratosis congenita. Nature **413:**432–435.
46. **Vulliamy, T., A. Marrone, R. Szydlo, A. Walne, P. J. Mason, and I. Dokal.** 2004. Disease anticipation is associated with progressive telomere shortening in families with dyskeratosis congenita due to mutations in TERC. Nat. Genet. **36:**447–449.
47. **Vulliamy, T. J., A. Walne, A. Baskaradas, P. J. Mason, A. Marrone, and I. Dokal.** 2005. Mutations in the reverse transcriptase component of telomerase (TERT) in patients with bone marrow failure. Blood Cells Mol. Dis. **34:**257–263.
48. **Wang, F., E. R. Podell, A. J. Zaug, Y. Yang, P. Baciu, T. R. Cech, and M. Lei.** 2007. The POT1-TPP1 telomere complex is a telomerase processivity factor. Nature **445:**506–510.
49. **Watson, J. M., and D. E. Shippen.** 2007. Telomere rapid deletion regulates telomere length in *Arabidopsis thaliana*. Mol. Cell. Biol. **27:**1706–1715.
50. **Xin, H., D. Liu, M. Wan, A. Safari, H. Kim, W. Sun, M. S. O'Connor, and Z. Songyang.** 2007. TPP1 is a homologue of ciliate TEBP-beta and interacts with POT1 to recruit telomerase. Nature **445:**559–562.
51. **Yamaguchi, H., R. T. Calado, H. Ly, S. Kajigaya, G. M. Baerlocher, S. J. Chanock, P. M. Lansdorp, and N. S. Young.** 2005. Mutations in TERT, the gene for telomerase reverse transcriptase, in aplastic anemia. N. Engl. J. Med. **352:**1413–1424.